

EFFECTS OF MULTIPLE DOSES OF SIMVASTATIN AND ARTESUNATE MONOTHERAPY ON *Schistosoma mansoni* ADULT WORMS DURING INFECTION IN HYPERLIDEMIC MICE

Alba Cristina Miranda de Barros Alencar¹, Thaís Silva dos Santos², Luciana Brandão-Bezerra², Eduardo José Lopes-Torres², José Firmino Nogueira-Neto³, Renata Heisler Neves² and José Roberto Machado-Silva²

ABSTRACT

A single dose of simvastatin and of artesunate monotherapy cause damage to the reproductive system of schistosomes as well as severe tegumental damage in male worms recovered from mice fed high-fat chow. This study aims to investigate whether treatment with multiple-dose regimes may offer more antischistosomal activity advantages than single daily dosing in mice fed high-fat chow. For this purpose, nine weeks post-infection, Swiss Webster mice were gavaged with simvastatin (200 mg/kg) or artesunate (300 mg/kg) for five consecutive days and euthanized two weeks post-treatment. Adult worms were analyzed using brightfield microscopy, confocal microscopy and scanning electron microscopy, presenting damages caused by simvastatin and artesunate to the reproductive system of males and females as well as tegument alterations, including peeling, sloughing areas, loss of tubercles, tegumental bubbles and tegument rupture exposing subtegumental tissue. The overall findings in this study revealed the potential antischistosomal activity of simvastatin and artesunate against *Schistosoma mansoni* adult worms, in addition to showing that multiple doses of either monotherapy caused severe damage to the tegument.

KEY WORDS: *Schistosoma mansoni*; hyperlipidemia; simvastatin; artesunate; microscopy.

1. Fluminense Federal University, Medical School, Department of Pathology, Rio de Janeiro, Brazil.

2. State University of Rio de Janeiro, Faculty of Medical Sciences, Biomedical Center, Department of Microbiology, Immunology and Parasitology Romero, Lascasas Porto Laboratory of Helminthology, Rio de Janeiro, Brazil.

3. State University of Rio de Janeiro, Faculty of Medical Science, Biomedical Center, Lipid Laboratory, Rio de Janeiro, Brazil.

Alba Cristina Miranda de Barros Alencar - ORCID: <https://orcid.org/0000-0002-0473-4381>, Thaís Silva Santos - ORCID: <https://orcid.org/0000-0002-0233-6240>, Luciana Brandão-Bezerra - ORCID: <https://orcid.org/0000-0001-6729-8487>, Eduardo José Lopes-Torres - ORCID: <https://orcid.org/0000-0003-0206-3681>, José Firmino Nogueira Neto - ORCID: <https://orcid.org/0000-0002-5368-5248>, Renata Heisler Neves - ORCID: <https://orcid.org/0000-0002-5442-0030>, José Roberto Machado Silva - ORCID: <https://orcid.org/0000-0003-3085-0228>

Corresponding author: Alba Cristina Miranda de Barros Alencar. E-mail: acmbalencar@id.uff.br

Received for publication: 21/12/2020. Reviewed: 26/2/2021. Accepted: 27/2/2021.

INTRODUCTION

Schistosomiasis is the second most prevalent among the group of neglected tropical diseases (NTDs) (CDC, 2018). Intestinal schistosomiasis caused by a blood-dwelling flatworm *Schistosoma mansoni* is a chronic parasitic disease entailing a substantial burden on human health in poor communities from Sub-Saharan Africa, Latin America, and the Caribbean islands without access to safe water, sanitation, and hygiene (WASH) (Campbell et al., 2014; CDC, 2018).

Mammal hosts (humans, non-human hosts and rodents) become infected through skin contact with water bodies contaminated with cercariae (infectious larval stage) released by freshwater snails of the genus *Biomphalaria*. Once inside the host, the cercaria undergoes complex morphological and biochemical transformations to schistosomula which migrates from the skin to the lungs and then to the liver, where it matures into an adult egg-laying parasite. At 5-6 weeks mated worms move to the mesenteric vessels, where females release immature eggs (Andrade, 2009), which become mature by passing through the mammalian intestinal wall. Eggs reach the gut lumen and are excreted with host feces into the environment. Subsequently, eggs hatching in freshwater originate a ciliated larva (miracidium) that infects species of *Biomphalaria*, thus completing the life cycle (Costain et al., 2018).

Current treatment for schistosomiasis mansoni relies on praziquantel (PZQ) monotherapy, but the exact molecular mechanism is not well understood (Bergquist & Elmorshedy, 2018; Thomas & Timson, 2018). The development of drug-resistance has become an issue of utmost concern due to its mass administration (Cioli et al., 2014; Neves et al., 2015; Lago et al., 2018; Pereira et al., 2019), as well as low efficacy against juvenile stages (Doenhoff et al., 2009). This concern has motivated researchers to discover new effective antischistosomal drugs (reviewed in Caffrey et al., 2019), or new alternatives for the treatment of schistosomiasis (reviewed in Adekiya et al., 2020). In the latter context, drug repositioning is a strategy used to identify new uses for marketed drugs (Giuliani et al., 2018; Gouveia et al., 2018).

Artemisinin (qinghaosu) is a compound derived from the Chinese plant *Artemisia annua* L, long known due to its fever reducing characteristic (Weathers et al., 2014). Aside from its antimalarial activity, several studies assessed the efficacy of artemisinin (ART) and its derivatives (artemether and artesunate) against *S. mansoni* in animal models (Utzinger et al., 2001).

Morphological and biological studies of this parasite have shown that the tegument and the reproductive organs are potential drug targets. In addition, 7-day-old schistosomula are more susceptible to a single dose of artemether than 21-day-old parasites (El-Beshbishi et al. 2013).

ART administered at the patent infection (45-49 dpi) reduced schistosome body size, induced worm shift, female burden tissue egg load and morphological changes which were seen in both the reproductive organs (vitelline glands and ovary) and oogram (Araújo et al., 1991; Abdul-Ghani et al., 2011; El-Beshbishi et al., 2013).

Artesunate (AS) given to mice at 300 mg/kg during the pre-patent phase revealed that older schistosomula (23 dpi) are more susceptible than younger (15dpi). Along with this, AS can hinder the maturing stage of schistosomula, as revealed by alterations in the structural characteristic of their gut (schistogram) (Vimieiro et al., 2013). Moreover, AS administered 45 dpi in a single dose of 300 mg/kg also showed activity by reducing worm recovery, inducing death of hepatic worms and oogram changes. Drug-induced morphological damages were characterized by alterations of reproductive organs (cellular alterations in vitelline glands and reduced ovary). In addition, oral administration of 300 mg/kg for five consecutive days induced greater hepatic shift and worm death compared to the single dose (Araújo et al., 1999).

Statins are a family of drugs widely used as cholesterol lowering agents (Wang et al., 2008; Rutishauser, 2011), as well as their pleiotropic functions such as antischistosomal agent *in vitro* (Rojo-Arreola et al., 2014). *In vivo* studies have shown that lovastatin administered during five consecutive days reduced female schistosome maturation, altered reproductive organs and egg production with oogram changes in mice fed normal chow (Araújo et al., 2002, 2008).

The impact of the association between diet composition and experimental schistosomiasis mansoni has been recently reviewed (Marques et al., 2018). Our team has shown that in a cholesterol-rich environment, schistosomes increase fertility and egg maturity (Neves et al., 2007a). Besides all of the reasons aforementioned of limitations in the schistosomicidal drug's efficacy, the role of the host diet on the chemotherapeutic treatment is lacking (Augusto et al., 2019). We recently demonstrated that a single dose of simvastatin (200 mg/kg) and artesunate (300 mg/kg) alone caused consistent damage to the reproductive system of schistosomes (testicular lobes, vitelline glands and ovarian cells), as well as severe tegumental damage in male worms in mice fed high-fat chow (Alencar et al., 2016). In view of such results, we investigated whether treatment with multiple-dose regimes may offer any antischistosomal activity advantage in relation to a single daily dose in mice fed high-fat chow.

MATERIAL AND METHODS

Ethics statement

Animal care and experimental protocol complied with the Guidelines for the Care and Use of Laboratory Animals [National Research Council (US) Committee for the Update of the Guidelines for the Care and Use of Laboratory Animals, 2011], the Brazilian Law 11.794/2008 and the regulations of the National Council of Animal Experimentation Control (CONCEA). The Animal Care and Use Committee of the Biology Institute of the State University of Rio de Janeiro approved the experimental guideline (process number: CEUA/013/2013).

Experimental design

Females Swiss Webster (SW), three weeks of age, were obtained from the Laboratory Animal Breeding Center (Oswaldo Cruz Foundation, Rio de Janeiro, Brazil). Mice were housed in propylene cages (40x33cm) under a controlled environment (21 ± 1 °C, humidity $60 \pm 10\%$, and 12 h /12 h dark/light cycle), with free access to food and water throughout the experiment.

Mice were fed high-fat chow (HFC), containing lard, egg yolk, wheat flour, corn starch, casein and vitamins and minerals (47% carbohydrates, 24% proteins, 29% lipids) (5.7 kcal/g body mass/day) for six months, starting from 21 days of life (weaning) (Neves et al., 2006). Mice were fed a standard mouse chow pellet (Nuvilab CR-I-NUVITAL Nutrients Ltda®. Paraná, Brazil) as the control group.

After six months on the designated diets (Neves et al., 2007a), the mice (n=52) were infected subcutaneously with 80 *S. mansoni* cercariae (BH strain, Brazil), as previously described (Martinez et al., 2003). Cercariae were obtained from the Laboratory of Malacology (Oswaldo Cruz Institute, FIOCRUZ, Rio de Janeiro State, Brazil).

Treatment schedule and experimental groups

Mice were given simvastatin® (Medley, Campinas, São Paulo, Brazil) or artesunate® (Farmanguinhos, FIOCRUZ, Rio de Janeiro State, Brazil) dissolved in 1,000 µl water and 250 µl Cremophor® (Sigma Chemical Company, St. Louis, MO, USA) nine week pi. Mice were gavaged with simvastatin (200 mg/kg bw) or artesunate (300 mg/kg bw) for five consecutive days. The untreated group received 250 µl Cremophor also for five days.

The mice were allocated into six groups according to treatment and diet: USC: untreated, standard chow (n=7); SCS: standard chow treated with simvastatin, (n=9); SCA: standard chow treated with artesunate (n=11); UHFC: untreated, high-fat chow (n=8); HFCS: high-fat chow treated with simvastatin (n=9); HFCA: high-fat chow treated with artesunate (n=9).

Parasitological examination and cholesterol analysis

Fecal samples were collected from each mice group at week 6 post infection to monitor schistosome eggs (two slides per animal), using the Kato-Katz technique (Katz et al., 1972). At week 11, mice were euthanized by cervical dislocation.

The small intestine removed for oogram determination was cut into segments, each 1 cm in length, compressed between glass slides and examined through a light microscope (Olympus BX50 Miami, Florida, USA). Schistosome eggs were classified into mature, immature and dead (Prata, 1957). At least 100 eggs were evaluated for each animal.

After euthanasia, blood samples obtained by cardiac puncture were centrifuged at 2000 g for 15 min, and the serum was stored at -20 °C for further cholesterol analysis. Total cholesterol (TC) level was measured using a colorimetric enzymatic method, according to standard technique at Lipids Laboratory (Lablip, Policlínica Piquet Carneiro, State University of Rio de Janeiro, Rio de Janeiro, Brazil).

Recovery of worms

Adult worm burden was determined after removing from the portal system and mesenteric veins for counting and sexing under a stereomicroscope. The percentage of reduction for each treated group was determined with the following formula: $P = (\text{number of worms recovered from the control group} - \text{number of worms recovered from the treated group}) / (\text{number of worms from the control group}) \times 100$ (Cioli et al., 2004).

Morphological and morphometric examination

Adult worms were prepared using the conventional protocol for light and confocal microscopy, as previously described (Neves et al., 2007a). Briefly, fixation with AFA solution (95% alcohol, 3% formaldehyde and 2% glacial acetic acid) at room temperature, staining with hydrochloric carmine (2.5%), dehydration in a graded ethanol series (70°GL, 90°GL and absolute), clarification with methyl salicylate and mounting on microscope slides with Canada balsam (1:2).

Whole-mounted specimens from USC (n=46), SCS (n=46), SCA (n=39), UHFC (n=57), HFCS (n=46) and HFCA (n=20) were analyzed by light microscopy (LM), using a light microscope (Olympus BX41, Miami, Florida, USA), coupled to a digital camera (Sony, Tokyo, Japan) at the Romero Lascasas Porto Laboratory of Helminthology, Faculty of Medical Sciences, UERJ (Neves et al., 1998). Morphometric analysis was performed with a computer imaging analysis software (Image Pro Plus, Media Cybernetics, USA). The measurements included male reproductive organ (germ cells density in testicular lobes), tegument thickness, and tubercles height. All densities were analyzed on a scale, in which three crosses (+++) represent normal pattern, two (++) or one cross (+) indicate reduced density (Brandão-Bezerra et al., 2019).

The reproductive organs of twenty specimens from each group (10 males and 10 females) previously analyzed by LM were also examined by confocal microscopy (CM), based on our previous procedures (Neves et al., 2004, 2007a; Alencar et al., 2016). Whole mounts were imaged using a Zeiss confocal microscope LSM 510–META (Zeiss, Germany), with a 543 nm He/Ne laser and a LP 570 filter under reflected mode (Brandão-Bezerra et al., 2019) at the Platform/Laboratory of Electron and Confocal Microscopy, UERJ.

Adult male worms collected for scanning electron microscopy (SEM) analysis were washed in saline solution, fixed with AFA and sputter-coated for 10 seconds with gold with 20-25nm thickness (Lopes-Torres et al., 2013). Samples were dehydrated in a graded ethanol series (70–100% Degree Gay Lussac) for 40 minutes at each step, critical-point dried in CO₂, mounted on metallic stubs and coated with gold (20–25 nm deposited). All SEM images were analyzed using the electron microscope Jeol/EO JSM-6510 (Jeol, Tokyo, Japan) at the Institute of Chemistry (State University of Rio de Janeiro, Rio de Janeiro, Brazil).

Statistical analysis

Data are expressed as mean ± standard error. Data were analyzed using the Statistical Package for the Social Sciences (SPSS) software. The groups were compared using the following tests: Mann-Whitney (tegument thickness and tubercles height), Student's T test (total cholesterol and worm recovery). The level of significance was set at $p \leq 0.05$.

RESULTS

Cholesterol analysis

Plasma total cholesterol levels are shown in Table 1. Cholesterol levels were increased in mice fed high-fat chow (UHFC, HFCS and HFCA) compared to mice fed standard chow (USC, SCS and SCA). Artesunate had no effect on reducing cholesterol levels (SCA, 73 ± 2.8 mg/dL; HFCA, 107 ± 6.1 mg/dL), compared to controls (USC, 66 ± 4.1 mg/dL; UHFC, 89 ± 3 mg/dL).

Parasitological analysis

Data on parasitological analysis are shown in Table 1. The worm recovery was approximately 2 to 4-fold lower in treated mice compared to untreated groups: USC (21 ± 5) and UHFC (24 ± 3). No statistical differences were observed in worm recovery (SCS, 12 ± 3 vs HFCS, 12 ± 2 ; SCA, 7 ± 1 vs HFCA, 5 ± 1). Although not significant, treatment with simvastatin (SCS, 24% and HFCS, 54%) or artesunate (SCA, 49% and HFCS, 73%) resulted in worm burden reduction.

Even though no major differences were found in testicular (germ) cell density when HFCS (93%) and HFCA (87%) were compared to SCS (94%) and SCA (90%), respectively (Table 1).

As shown in Table 1, mice fed high-fat chow (UHFC, 15 ± 0.8 μ m; HFCS, 9.9 ± 0.3 μ m) presented reduced tegumental thickness when compared to their respective diet groups (USC, 21 ± 1.7 μ m; SCS (11 ± 0.5 μ m). Likewise, the height of the tubercles was reduced in UHFC (5.9 ± 0.2 μ m) when compared to USC (8.2 ± 0.4 μ m) and HFCA (4.9 ± 0.1 μ m) compared to SCA (5.9 ± 0.2 μ m).

Morphological analysis

Morphological features of the reproductive system were investigated using confocal microscopy on whole-mount male worms (Figure. 1). Untreated worms (USC and UHFC) showed testicular lobes with rounded cells and visible nucleus. The seminal vesicle was filled with an abundant amount of sperm (Figure 1a and b). On the other hand, simvastatin induced morphological alterations in testicular lobes, irrespective of chow. Worms from the SCS group displayed immature germ cells and anucleated cells and low density of spermatozoa within the seminal vesicle (Figure 1c). In HFCS, similar changes were found, besides amorphous cells (Figure 1d). Artesunate also induced morphological alterations in the male reproductive organs. Immature, amorphous, granular nucleus, anucleated germ cells and immature cells and a low amount of sperm were found within the seminal vesicle in both SCA and HFCA groups (Figure 1e and f).

Table 1. Total cholesterol level and parasitological parameters in *Schistosoma mansoni*-infected mice fed standard chow or high-fat chow. Treatment with simvastatin (200 mg/kg) or artesunate (300 mg/kg) for five consecutive days.

Parameters	Groups					
	USC	SCS	SCA	UHFC	HFCS	HFCA
Total cholesterol (mg/dl)	66 ± 4.1	57 ± 3.8	73 ± 2.8	89 ± 3 ^a	83 ± 4.7 ^b	107 ± 6.1 ^c
Adult worm recovery	21 ± 5	12 ± 3	7 ± 1	24 ± 3	12 ± 2	5 ± 1
Worm burden reduction (%)	--	24	49	--	54	73
Worm morphology						
Germ cell density (%)	97	94	90	100	93	87
Tegument thickness (µm)	21 ± 1.7	11 ± 0.5	10 ± 1.1	15 ± 0.8 ^a	9.9 ± 0.3	10 ± 0.5
Tubercle height (µm)	8.2 ± 0.4	5.5 ± 0.2	5.9 ± 0.2	5.9 ± 0.2 ^a	5.3 ± 0.2	4.9 ± 0.1 ^c
Oogram (%)						
Immature	97	99	58	58	63	63
Mature	02	00	12	22	05	07
Dead	01	01	30	20	32	30

All data are represented as mean ± standard error. Significant differences ($p < 0.05$) when compared to group: USC (^a); SCS (^b); SCA (^c). USC: untreated, standard chow; SCS: standard chow treated with simvastatin; SCA: standard chow treated with artesunate; UHFC: untreated, high-fat chow; HFCS, high-fat chow treated with simvastatin. HFCA: high-fat chow treated with artesunate.

The female's reproductive organs analyzed by confocal are shown in Figure 2. Untreated females presented normal ovaries composed of round oocytes with visible nucleus and sperm-filled seminal receptacle (Figure 2a and b). In female schistosome, ovarian cells from the simvastatin-treated group (SCS) revealed changes in shape mostly anucleated cells or granular nuclei (Figure 2c). In addition, HFCS group presented ovary with triangular cells in shape (Figure 2d). Treatment with artesunate has caused more intense changes than simvastatin, regardless of diet. Several morphological alterations were observed, such as amorphous, triangular in shape and/or anucleated cells (Figure 2e and f).

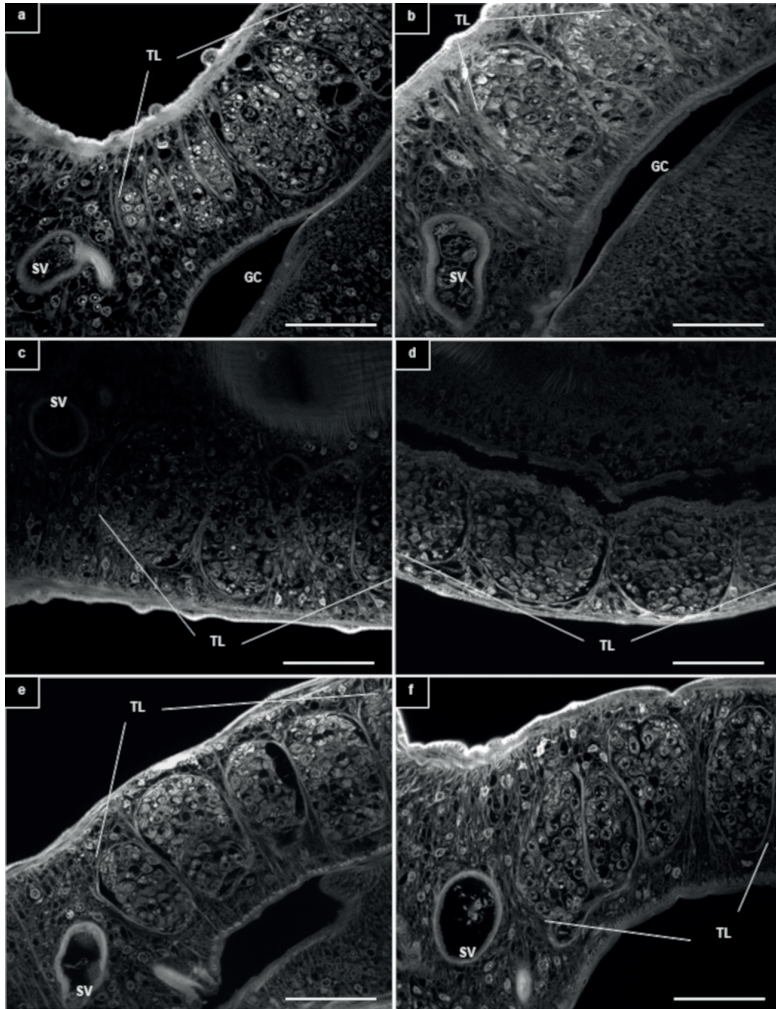


Figure 1. Confocal images showing testicular lobes and seminal vesicle on male *Schistosoma mansoni* collected from the mice fed standard (a, d, e) or high-fat chow (b, d, f). Mice were treated with simvastatin (c, d) or artesunate (e, f) for 5 consecutive days. Untreated worms showing gynaecophoric canal, cells with visible nucleus within the testicular lobes and seminal vesicle (a, b). Worms treated with simvastatin presented immature and anucleated germ cells in testicular lobes, sperm cells within the seminal vesicle (c) and amorphous and anucleated cells (d). Worms treated with artesunate showing testicular lobes with immature, amorphous cells with granular or anucleated nucleus and seminal vesicles with low immature cell density and sperm (e, f). Scale bars: 50 μ m. Abbreviations: gynaecophoric canal (GC), seminal vesicle (SV), TL: testicular lobes.

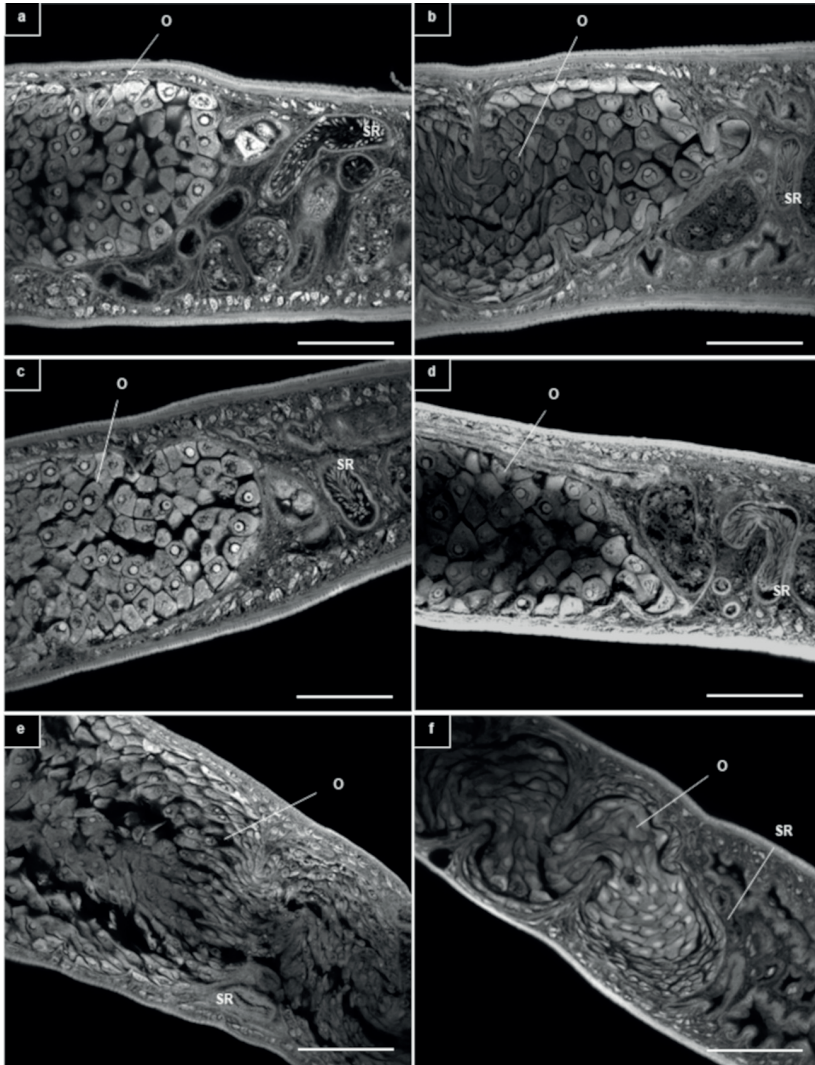


Figure 2. Confocal images showing reproductive organs on female *Schistosoma mansoni* collected from mice fed standard (a, c, e) or high-fat chow (b, d, f). Mice were treated with simvastatin (c, d) or artesunate (e, f) for five consecutive days. Untreated worms showing ovary with rounded oocytes with visible nucleus and spermatozoa within the seminal receptacle (a, b). Worms treated with simvastatin (SCS group), presenting ovary with amorphous anucleated cells or granular nuclei (c), triangular shape cells and sperm-filled seminal receptacle (d). Worms exposed to artesunate (SCA group) showing distorted ovary characterized by amorphous, triangular, elongated and/or anucleated cells and sperm-filled seminal receptacle (e, f). Scale bars: 50 μ m. Abbreviations: O: ovary; SR: seminal receptacle.

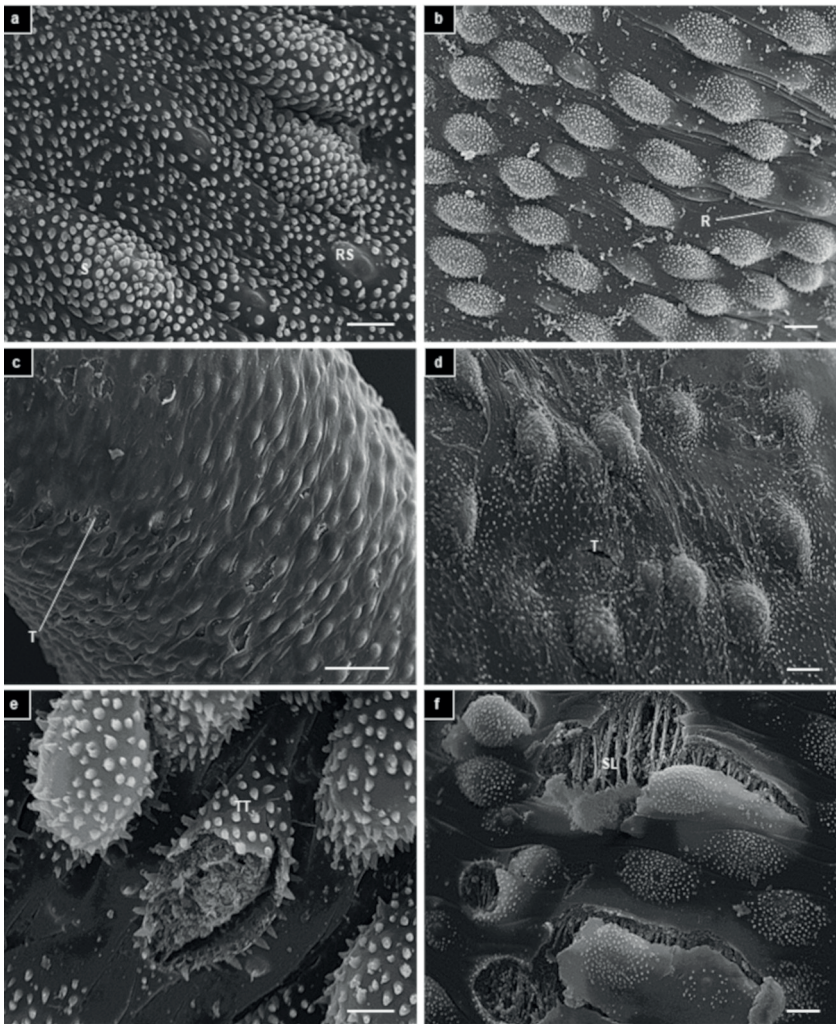


Figure 3. Scanning electron microscopy showing dorsal tubercles on adult male *Schistosoma mansoni* collected from mice fed standard chow (a, b). Untreated worms (USC group) showed typical surface topography with evenly distributed intact spiny tubercles, sensory receptor (a) and ridges (b). Treated worms with simvastatin for five consecutive days (SCS group) resulted in damaged tegument peeling (c) and damaged tubercles (d). Treatment with artesunate for five consecutive days (SCA) caused peeling on the outer layer with exposure of subtegumental tissue, and tubercle damage with loss of spines and tegument desquamation (e, f). Scale bars: (a, e) 5 μ m; (b, d, f) 10 μ m; (c) 50 μ m. Abbreviations: ridges (R), spines (S), subtegumentar layer (SL), tegument (T) and tubercles (TT).

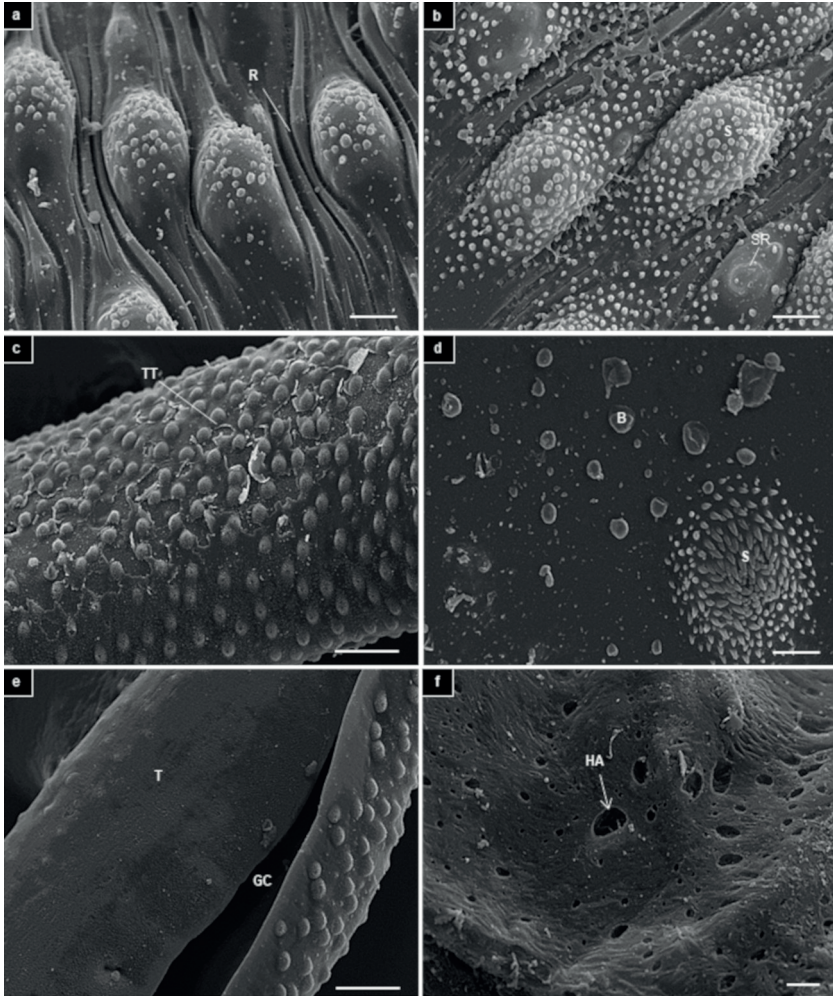


Figure 4. Scanning electron microscopy showing dorsal tubercles on adult male *Schistosoma mansoni* collected from mice fed high-fat chow. Untreated worms (UHFC group) exhibit intact tubercles with overlying spines, ridges (a) and sensory receptor (b). Worms treated with simvastatin for five consecutive days showed tegument peeling, some tubercles exhibit rupturing, desquamation (c) and tegumental bubbles (d). Worms treated with artesunate for five consecutive days showed a smooth area devoid of tubercles on one side of the gynaecophoric canal (e), pore-like structures on the tegument with different sizes (f). Scale bars: (a, b, d) 5 μ m; (f) 10 μ m; (c, e) 50 μ m. Abbreviations: bubbles (B), ridges (R), gynaecophoric canal (GC), hollow area (HA), sensory receptor (SR), spines (S), tegument (T) and tubercles (TT).

Scanning electron microscopy (SEM) images of adult male *S. mansoni* are shown in Figure 3 and 4. As expected, untreated worms from mice fed standard chow (USC) presented the typical surface topography with evenly distributed intact spiny tubercles, sensory receptor (Figure 3a) and ridges (Figure 3b). By contrast, the tegument was disrupted in worms subjected to simvastatin or artesunate over five consecutive days. SCS showed moderate tegument peeling, damaged tubercles with loss of spines (Figure 3c) and unevenly distributed tubercles covered by detached tissue (Figure 3d). Artesunate treatment (SCA) caused peeling on the outer layer with exposure of subtegumental tissue (Figure 3e) and tubercle damage with loss of spines (Figure 3f).

Similar to the USC group, untreated worms from mice fed high-fat chow (UHFC) showed typical surface topography with evenly distributed intact spiny tubercles, ridges (Figure 4a) and sensory receptor (Figure 4b). In the HFCS group, the surface topography was also altered with tegument peeling, some tubercles exhibited rupturing (Figure 4c) and tegumental bubbles (Figure 4d). In worms treated with artesunate (HFCA), many flattened tubercles and a smooth area devoid of tubercles in one of the folds of the gynaecophoric canal were found (Figure 4e). As well as the pitted appearance (like pores) of the tegument, hollow areas in different sizes were also found (Figure 4f).

DISCUSSION

A recent publication called into question whether host diet may play a role on chemotherapeutic treatment (Augusto et al., 2019). Concerning the present work, we addressed the effects of artesunate and simvastatin using a regimen in mice fed high-fat chow. Consistent with our previous reports (Neves et al., 2007a; Alencar et al., 2009, 2016; da Silva Filomeno et al., 2020), feeding high-fat chow (UHFC) increased levels of total cholesterol (TC) compared with that of standard chow-fed control mice (USC).

Previous studies demonstrated that both experimental (Doenhoff et al., 2002; Neves et al., 2007; Alencar et al., 2009; Stanley et al., 2009) and human schistosomiasis induce TC level reduction (Sanya et al., 2020) due to use of TC by adult worms. Given that simvastatin is a powerful TC lowering compound (Pose et al., 2019), TC levels reduction in mice fed high-fat chow (HFCS) would be expected. In fact, our results confirmed this. Beyond antimalarial action, artesunate shows pleiotropic activity by reducing TC levels either as a monotherapy or combination therapy in rabbits (Wang et al., 2013). In our experimental mice groups, artesunate-treated (SCA and HFCA) have not shown reduction in TC levels compared to controls (USC and UHFC).

Evidence indicates that host diet has an influence on the development of adult worms and over the course of *S. mansoni* infection (Marques et al., 2018). During the last few years, our group has shown that in a cholesterol-rich environment, schistosomes increase infectivity rate, fertility and egg maturity, when compared to worms kept on normal mouse chow (Neves et al., 2007a; Alencar et al., 2016). We here corroborate that high-fat feeding results in higher adult worm recovery (HFCS), but no statistical difference was found (Alencar et al., 2016).

Due to their blood habit, adult schistosomes may coexist with a large number of harmful factors (Skelly et al., 2014; Da'dara & Skelly, 2014; Blohm et al., 2016), including exposure to drugs with schistosomicidal activity (Augusto et al., 2019; Caffrey et al., 2019). In fact, previous studies have demonstrated that a multiple-dose lovastatin and artesunate regimen reduced total worm rates in mice fed standard mouse chow (Araújo et al., 1999, 2002). However, the use of these drugs in a multiple-dose regimen has not been reported so far in mice fed high-fat chow. The current findings provide evidence that both drugs reduced the worm burden by 54% (HFCS) or 73% (HFCA). It is interesting to contrast the results obtained here with our previous study using a single dose, in which artesunate-treated mice showed lower worm burden reduction (HFCA, 49%) (Alencar et al., 2016). This suggests that the long-term treatment could potentially increase the antischistosomal activity of artesunate, regardless of diet (Araújo et al., 1999; Shaohong et al., 2006).

The tegument is the primary surface for host-parasite interaction by providing, protection, immunomodulation and nutrient ingestion (Skelly et al., 2014). On the other hand, the tegument is target for antischistosomal compounds (Leow et al., 2014). Male specimens harbor numerous large spiny tubercles on the dorsal surface, which help the migration from liver to mesenteric vessels. Here, we found both reduced tegument thickness and tubercle height mainly due to artesunate, in line with our previous investigation (Alencar et al., 2016). The morphological features of untreated worms from mice fed control (USC) or high-fat chow (UHFC) exhibited a typically normal topographic morphology, including evenly distributed intact spiny tubercles, ridges and sensory receptor in agreement with previous reports (Utzinger et al., 2001; Keiser et al., 2015; Pinto-Almeida et al., 2016). Our SEM investigations revealed that all treated groups (SCS, SCA, HFCS and HFCA) displayed a variety of tegument changes, including peeling, sloughing areas, loss of tubercles, tegument rupture exposing subtegumental tissues and tegumental bubbles. These findings are worth highlighting. First, previous studies have shown that the tegument damage is a common feature with several schistosomicidal agents (Soliman & Ibrahim 2005; Alencar et al., 2016). Second, males with disrupted tegument can be vulnerable to the host's immune response (Skelly & Wilson, 2006; Reimers et al., 2015; Buchter et al., 2018), a factor that could have interfered with the rate of worm recovery.

In view of such results, we investigated whether long-term treatment would cause morphological alterations to male reproductive gonads. Indeed, the density of germ cells within the testicular lobes was reduced in the HFCS (-7%) and HFCA (-13%) groups, compared to the normal pattern in untreated worms (UHFC). Our findings extend earlier studies regarding testis alterations (Araújo et al., 2002). Having identified such alterations by light microscopy, we further analyzed the reproductive system using confocal microscopy. Consistent with our previous study, simvastatin (HFCS) and artesunate (HFCA) treatment induced morphological alterations in testicular lobes characterized by cellular disorganization, immature cells without sperm formation or low density of spermatozoa within the seminal vesicle, when compared to normal features observed in untreated worms (USC and UHFC) (Alencar et al., 2016).

Earlier investigations focused on the effects of artesunate and lovastatin monotherapy on egg production due to its relevance for both pathogenesis and disease transmission. In fact, both artesunate and lovastatin caused disorganization of gonadal tissue structures (ovary and vitelline follicles) in female worms collected from mice fed standard chow (Araújo et al., 1999, 2002). Here, we show that the multiple dose regimen of simvastatin and artesunate treatment also led to detrimental effects on the reproductive organs, consistent with our data, when administered as a single dose (Alencar et al., 2016). It is likely that oogram changes characterized by decreased immature eggs and increased dead eggs and egg burden reduction (data not shown) are associated with gonad damages (Araújo et al. 1999, 2002; Shaohong et al., 2006).

Our study focused on the role of host diet on the schistosomiasis treatment, which is a promising new area of research. Taken together, our findings indicate that simvastatin and artesunate display activity against adult schistosomes in mice under hyperlipidemic condition.

ACKNOWLEDGEMENTS

The authors are grateful to Kíssila Rabelo at the Platform/Laboratory of Electron and Confocal Microscopy at the State University of Rio de Janeiro for confocal microscopy facilities, Marcia Christina Amorim Moreira Leite and Isaac Albert Mallet at the Electron Microscopy Laboratory, Institute of Chemistry, State University of Rio de Janeiro, Brazil, for help in processing samples. All authors are grateful to Vania Pinto at the Laboratory of Lipids (LabLip) Faculty of Medical Science, State University of Rio de Janeiro, Rio de Janeiro, Brazil for biochemical determinations. The authors would like to thank the Malacology Laboratory at the Oswaldo Cruz Institute, for providing *S. mansoni* cercariae.

This study was sponsored by the National Council for Scientific and Technological Development (Conselho Nacional de Pesquisa e Desenvolvimento Tecnológico, CNPq, grant 480102/2013-9) and State of Rio de Janeiro Carlos Chagas Filho Research Foundation (Fundação Carlos Chagas Filho de Amparo à Pesquisa do Estado do Rio de Janeiro, FAPERJ, grants E-26/190.311/2012/E-26.210.034/2014) to JRMS. JRMS was also sponsored by a research fellowship from CNPq (304898/2012-2). ACMBA received a CNPq fellowship (142153/2011-7). EJLT is sponsored by a research fellowship from FAPERJ (JCNE E-26/202.660/2018). The funders had no role in study design, data collection and analysis, decision to publish, or preparation of the manuscript.

CONFLICTS OF INTEREST

The authors declare no conflict of interest.

REFERENCES

1. Abdul-Ghani R, Loutfy N, Sheta M, Hassan A. Chemotherapeutic efficacy of a natural combination in the treatment of mansonic schistosomiasis: An experimental study. *Res Rep Trop Med* 2: 1-7, 2011.
2. Adekiya TA, Kondiah PPD, Choonara YE, Kumar P, Pillay V. A review of nanotechnology for targeted anti-schistosomal therapy. *Front Bioeng Biotechnol* 8: 32, 2020.
3. Alencar ACM de B, Neves RH, Águila MB, Mandarim-de-Lacerda CA, Gomes DC, Machado-Silva JR. High fat diet has a prominent effect upon the course of chronic schistosomiasis mansoni in mice. *Mem Inst. Oswaldo Cruz* 104: 608-613, 2009.
4. Alencar ACM de B, Santos T da S, Neves RH, Lopes-Torres EJ, Nogueira-Neto JF, Machado-Silva JR. Simvastatin and artesunate impact the structural organization of adult *Schistosoma mansoni* in hypercholesterolemic mice. *Exp Parasitol* 167: 115-123, 2016.
5. Andrade ZA. Schistosomiasis and liver fibrosis. *Parasite Immunol* 31: 656-663, 2009.
6. Araújo N, Kohn A, Katz N. Activity of the artemether in experimental schistosomiasis mansoni. *Mem Inst Oswaldo Cruz* 86: 185-188, 1991.
7. Araújo N, Kohn A, Katz N. Avaliação terapêutica do artesunato na infecção experimental pelo *Schistosoma mansoni*. *Rev Soc Bras Med Trop* 32: 7-12, 1999.
8. Araújo N, Kohn A, Oliveira AA de, Katz N. *Schistosoma mansoni*: the action of lovastatin on the murine model. *Rev Soc Bras Med Trop* 35: 35-38, 2002.
9. Araújo N, Mattos ACA, Sarvel AK, Coelho PMZ, Katz, N. Oxamniquine, praziquantel and lovastatin association in the experimental Schistosomiasis mansoni. *Mem Inst Oswaldo Cruz* 103: 450-454, 2008.
10. Augusto R de C, Duval D, Grunau C. Effects of the environment on developmental plasticity and infection success of *Schistosoma* parasites – An epigenetic perspective. *Front Microbiol* 10: 1475, 2019.
11. Bergquist R, Elmorshedy H. Artemether and praziquantel: Origin, mode of action, impact, and suggested application for effective control of human schistosomiasis. *Trop Med Infect Dis* 3: 125, 2018.
12. Blohm AS, Mäder P, Quack T, Lu Z, Hahnel S, Schlitzer M, Grevelding CG. Derivatives of biarylalkyl carboxylic acid induce pleiotropic phenotypes in adult *Schistosoma mansoni* in vitro. *Parasitol Res* 115: 3831-3842, 2016.

13. Brandão-Bezerra L, Martins JSC de C, de Oliveira RMF, Lopes-Torres EJ, Neves RH, Corrêa CL, Machado-Silva JR. Long-term ethanol intake causes morphological changes in *Schistosoma mansoni* adult worms in mice. *Exp Parasitol* 203: 30-35, 2019.
14. Buchter V, Hess J, Gasser G, Keiser J. Assessment of tegumental damage to *Schistosoma mansoni* and *S. haematobium* after in vitro exposure to ferrocenyl, ruthenocenyl and benzyl derivatives of oxamniquine using scanning electron microscopy. *Parasit Vectors* 11: 580, 2018.
15. Caffrey CR, El, Sakkary N, Mäder P, Krieg R, Becker K, Schlitzer M, Drewry DH, Vennerstrom JL, Grevelding CG. Drug Discovery and Development for Schistosomiasis. In: Swinney D, Pollastri M, Mannhold R, Buschmann H, Holenz J. (ed). *Neglected Tropical Diseases: Drug Discovery and Development. Wiley Online Library* 2019: 187-225, 2019.
16. Campbell SJ, Savage GB, Gray DJ, Atkinson J-AM, Soares Magalhães RJ, Nery SV, McCarthy JS, Velleman Y, Wicken JH, Traub RJ, Williams GM, Andrews RM, Clements ACA. Water, Sanitation, and Hygiene (WASH): A critical component for sustainable soil-transmitted helminth and schistosomiasis control. *PLoS Negl Trop Dis* 8: e2651, 2014.
17. CDC. Centers for Disease Control and Prevention. *Parasites - Schistosomiasis*, 2018. Available in: <https://www.cdc.gov/parasites/schistosomiasis/>. Accessed in: 8/5/2020.
18. Cioli D, Botros SS, Wheatcroft-Francklow K, Mbaye A, Southgate V, Tchuem Tchuente LA, Pica-Mattoccia L, Troiani AR, Seif El-Din SH, Sabra ANA, Albin J, Engels D, Doenhoff MJ. Determination of ED50 values for praziquantel in praziquantel-resistant and -susceptible *Schistosoma mansoni* isolates. *Int J Parasitol* 34: 979-987, 2004.
19. Cioli D, Pica-Mattoccia L, Basso A, Guidi A. Schistosomiasis control: Praziquantel forever? *Mol Biochem Parasitol* 195: 23-29, 2014.
20. Costain AH, MacDonald AS, Smits HH. Schistosome egg migration: Mechanisms, pathogenesis and host immune responses. *Front Immunol* 9: 3042, 2018.
21. Da'dara AA, Skelly PJ. Schistosomes versus platelets. *Thromb Res* 134: 1176-1181, 2014.
22. da Silva Filomeno CE, Costa-Silva M, Corrêa CL, Neves RH, Mandarim-de-Lacerda CA, Machado-Silva JR. The acute schistosomiasis mansoni ameliorates metabolic syndrome in the C57BL/6 mouse model. *Exp Parasitol* 212: 107889, 2020.
23. Doenhoff MJ, Stanley RG, Griffiths K, Jackson CL. An anti-atherogenic effect of *Schistosoma mansoni* infections in mice associated with a parasite-induced lowering of blood total cholesterol. *Parasitology* 125: 415-421, 2002.
24. Doenhoff MJ, Hagan P, Cioli D, Southgate V, Pica-Mattoccia L, Botros S, Coles G, Tchuem Tchuente LA, Mbaye A, Engels D. Praziquantel: Its use in control of schistosomiasis in sub-Saharan Africa and current research needs. *Parasitology* 136: 1825-1835, 2009.
25. El-Beshbishi SN, Taman A, El-Malky M, Azab MS, El-Hawary AK, El-Tantawy DA. In vivo effect of single oral dose of artemether against early juvenile stages of *Schistosoma mansoni* Egyptian strain. *Exp Parasitol* 135: 240-245, 2013.
26. Giuliani S, Silva AC, Borba JVV, Ramos PIP, Paveley RA, Muratov EN, Andrade CH, Furnham N. Computationally-guided drug repurposing enables the discovery of kinase targets and inhibitors as new schistosomicidal agents. *PLOS Comput Biol* 14: e1006515, 2018.
27. Gouveia M, Brindley P, Gärtner F, Costa J, Vale N. Drug repurposing for schistosomiasis: Combinations of drugs or biomolecules. *Pharmaceuticals* 11: 15, 2018.
28. Katz N, Chaves A, Pellegrino J. A simple device for quantitative stool thick-smear technique in schistosomiasis mansoni. *Rev Inst Med Trop Sao Paulo* 14: 397-400, 1972.
29. Keiser J, Panic G, Vargas M, Wang C, Dong Y, Gautam N, Vennerstrom JL. Aryl hydantoin Ro 13-3978, a broad-spectrum antischistosomal. *J Antimicrob Chemother* 70: 1788-1797, 2015.
30. Lago EM, Xavier RP, Teixeira TR, Silva LM, da Silva Filho AA, de Moraes J. Antischistosomal agents: state of art and perspectives. *Future Med Chem* 10: 89-120, 2018.

31. Leow CY, Willis C, Osman A, Mason L, Simon A, Smith BJ, Gasser RB, Jones MK, Hofmann A. Crystal structure and immunological properties of the first annexin from *Schistosoma mansoni*: insights into the structural integrity of the schistosomal tegument. *FEBS J* 281: 1209-1225, 2014.
32. Lopes-Torres EJ, de Souza W, Miranda K. Comparative analysis of *Trichuris muris* surface using conventional, low vacuum, environmental and field emission scanning electron microscopy. *Vet Parasitol* 196: 409-416, 2013.
33. Marques DVB, Felizardo AA, Souza RLM, Pereira AAC, Gonçalves RV, Novaes RD. Could diet composition modulate pathological outcomes in schistosomiasis mansoni? A systematic review of *in vivo* preclinical evidence. *Parasitology* 145: 1127-1136, 2018.
34. Martinez EM, Neves RH, de Oliveira RMF, Machado-Silva JR, Rey, L. Parasitological and morphological characteristics of Brazilian strains of *Schistosoma mansoni* in *Mus musculus*. *Rev Soc Bras Med Trop* 36: 557-564, 2003.
35. Neves B, Andrade C, Cravo P. Natural products as leads in schistosome drug discovery. *Molecules* 20: 1872-1903, 2015.
36. Neves RH, dos Santos Pereira MJ, de Oliveira RMF, Gomes DC, Machado-Silva JR. *Schistosoma mansoni* Sambon, 1907: Morphometric differences between adult worms from sympatric rodent and human isolates. *Mem Inst Oswaldo Cruz* 93: 309-312, 1998.
37. Neves RH, Costa-Silva M, Martinez EM, Branquinho TB, de Oliveira RMF, Lenzi HL, Gomes DC, Machado-Silva JR. Phenotypic plasticity in adult worms of *Schistosoma mansoni* (Trematoda: Schistosomatidae) evidenced by brightfield and confocal laser scanning microscopies. *Mem Inst Oswaldo Cruz* 99: 131-136, 2004.
38. Neves RH, Alencar ACM de B, Águila MB, Mandarim-de-Lacerda CA, Machado-Silva JR, Gomes DC. Somatic, biochemical and hepatic alterations in wild type mice chronically fed high fat diet. *Int J Morphol* 24: 625-632, 2006.
39. Neves RH, Alencar ACM de B, Águila MB, Mandarim-de-Lacerda CA, Machado-Silva JR, Gomes DC. Light and confocal microscopic observations of adult *Schistosoma mansoni* from mice fed on a high-fat diet. *J Helminthol* 81: 361-368, 2007a.
40. Neves RH, Alencar ACM. de B, Costa-Silva M, Águila MB, Mandarim-de-Lacerda CA, Machado-Silva JR, Gomes DC. Long-term feeding a high-fat diet causes histological and parasitological effects on murine schistosomiasis mansoni outcome. *Exp Parasitol* 115: 324-332, 2007b.
41. Pereira ASA, Silveira GO, Amaral MS, Almeida SMV, Oliveira JF, Lima MCA, Verjovski-Almeida S. *In vitro* activity of aryl-thiazole derivatives against *Schistosoma mansoni* schistosomula and adult worms. *PLoS One* 14: e0225425, 2019.
42. Pinto-Almeida A, Mendes T, de Oliveira RN, Corrêa S de AP, Allegretti SM, Belo S, Tomás A, Anibal F de F, Carrilho E, Afonso A. Morphological characteristics of *Schistosoma mansoni* PZQ-resistant and -susceptible strains are different in presence of praziquantel. *Front Microbiol* 7: 594, 2016.
43. Pose E, Trebicka J, Mookerjee RP, Angeli P, Ginès P. Statins: Old drugs as new therapy for liver diseases? *J Hepatol* 70: 194-202, 2019.
44. Prata A. Tipos de ovos de *Schistosoma mansoni*. In: Biópsia retal na esquistossomose mansoni. Serviço Nacional de Educação Sanitária: Rio de Janeiro, 1957. p.15-60.
45. Reimers N, Homann A, Höschler B, Langhans K, Wilson RA, Pierrot C, Khalife J, Grevelding CG, Chalmers IW, Yazdanbakhsh M, Hoffmann KF, Hokke CH, Haas H, Schramm G. Drug-induced exposure of *Schistosoma mansoni* antigens SmCD59a and SmKK7. *PLoS Negl Trop Dis* 9: e0003593, 2015.
46. Rojo-Arreola L, Long T, Asarnow D, Suzuki BM, Singh R, Caffrey CR. Chemical and genetic validation of the statin drug target to treat the helminth disease, Schistosomiasis. *PLoS One* 9: e87594, 2014.

47. Rutishauser J. Statins in clinical medicine. *Swiss Med Wkly* 141: 1-9, 2011.
48. Sanya RE, Webb EL, Zziwa C, Kizindo R, Sewankambo M, Tumusiime J, Nakazibwe E, Oduru G, Niwagaba E, Nakawungu PK, Kabagenyi J, Nassuuna J, Walusimbi B, Andia-Biraro I, Elliott AM. The effect of helminth infections and their treatment on metabolic outcomes: Results of a cluster-randomized trial. *Clin Infect Dis* 71: 601-613, 2020.
49. Shaohong L, Kumagai T, Qinghua A, Xiaolan Y, Ohmae H, Yabu Y, Siwen L, Liyong W, Maruyama H, Ohta N. Evaluation of the anthelmintic effects of artesunate against experimental *Schistosoma mansoni* infection in mice using different treatment protocols. *Parasitol Int* 55: 63-68, 2006.
50. Skelly PJ, Wilson RA. Making sense of the schistosome surface. *Adv Parasitol* 63: 185-284, 2006.
51. Skelly PJ, Da'dara AA, Li XH, Castro-Borges W, Wilson RA. Schistosome feeding and regurgitation. *PLoS Pathog* 10: 8, 2014.
52. Soliman MFM, Ibrahim MM. Antischistosomal action of atorvastatin alone and concurrently with medroxyprogesterone acetate on *Schistosoma haematobium* harboured in hamster: Surface ultrastructure and parasitological study. *Acta Trop* 93: 1-9, 2005.
53. Stanley RG, Jackson CL, Griffiths K, Doenhoff MJ. Effects of *Schistosoma mansoni* worms and eggs on circulating cholesterol and liver lipids in mice. *Atherosclerosis* 207: 131-138, 2009.
54. Thomas CM, Timson DJ. The mechanism of action of praziquantel: Six hypotheses. *Curr Top Med Chem* 18: 1575-1584, 2018.
55. Utzinger J, Shuhua X, N'Goran EK, Bergquist R, Tanner M. The potential of artemether for the control of schistosomiasis. *Int J Parasitol* 31: 1549-1562, 2001.
56. Vimieiro ACS, Araújo N, Katz N, Kusel JR, Coelho PMZ. Schistogram changes after administration of antischistosomal drugs in mice at the early phase of *Schistosoma mansoni* infection. *Mem Inst Oswaldo Cruz* 108: 881-886, 2013.
57. Wang CY, Liu PY, Liao JK. Pleiotropic effects of statin therapy: Molecular mechanisms and clinical results. *Trends Mol Med* 14: 37-44, 2008.
58. Wang YL, Wang ZJ, Shen HL, Yin M, Tang KX. Effects of artesunate and ursolic acid on hyperlipidemia and its complications in rabbit. *Eur J Pharm Sci* 50: 366-37, 2013.
59. Weathers PJ, Jordan NJ, Lasin P, Towler MJ. Simulated digestion of dried leaves of *Artemisia annua* consumed as a treatment (pACT) for malaria. *J Ethnopharmacol* 151: 858-863, 2014.